

International Conference on Space Optics—ICSO 2018

Chania, Greece

9–12 October 2018

Edited by Zoran Sodnik, Nikos Karafolas, and Bruno Cugny



UFSS (ultra fine sun sensor): CCD sun sensor with sub-arc second accuracy for the next solar observing satellite SOLAR-C

K. Tsuno

S. Wada

T. Ogawa

T. Shimizu

et al.



icso proceedings



UFSS (Ultra Fine Sun Sensor) – CCD sun sensor with sub-arcsecond accuracy for the next solar observing satellite SOLAR-C

K. Tsuno^{*a}, S. Wada^a, T. Ogawa^a, T. Shimizu^b, T. Hasegawa^b, M. Kubo^c,
H. Murao^d, S. Mizumoto^d, S. Fujishima^d, K. Toyonaga^d

^aRIKEN, 2-1, Hirosawa, Wako-shi, Saitama, Japan 351-1298; ^bJAXA/ISAS, 3-1-1, Yoshinodai, Chuo-ku, Sagami-hara-shi, Kanagawa, Japan 252-5210; ^cNational Astronomical Observatory of Japan, 2-21-1, Osawa, Mitaka-shi, Tokyo, Japan 181-8588; ^dMEISEI Electric Co. Ltd., 2223 Naganumamachi, Isesaki-shi, Gunma, Japan 372-8585

ABSTRACT

The Ultra Fine Sun Sensor (UFSS) on board the HINODE solar observing satellite is one of the most successful sun sensors. It is the linear CCD sun sensor with a special detection method using multiple slits, called the periodic reticle. The angular resolution of 0.14 arcsec in the noise equivalent angle (NEA) and 1 arcsec stability were achieved by the sensor head, of 1.2 kg weight. The concept of the detection method and processing algorithm of the Sun's direction is described. The system is modeled and the dynamic response of the system is characterized by the first-order lag system. By utilizing this characteristic, a resolution improvement three times higher can be expected by adjusting the parameters with a small modification to the HINODE UFSS processing algorithm. The design for a new UFSS for the next generation solar observation satellite, SOLAR-C, shall include these modifications. The thermomechanical design is also reviewed to improve stability and a design policy is obtained.

Keywords: CCD, Sun Sensor, YOHKO, HINODE

1. INTRODUCTION

The Ultra Fine Sun Sensor (UFSS), comprising a 1.2 kg sensor head, is the linear CCD sun sensor and utilizes a special detection method that involves multiple slits, called the periodic reticle. HINOTORI, YOHKO, and HINODE are a series of Japanese solar observing satellites. As the generations have progressed, improvement of the angular resolution of the instruments has been achieved, requiring a better pointing resolution and stability. The idea of the UFSS was devised to satisfy the requirement of a high-precision attitude sensor referring to the Sun in the YOHKO project^[1]. In this case, the angular resolution was limited to 2 arcsec, which corresponds to a timing resolution determined by the speed of the logic device of 1980s.

For the HINODE project, the sun sensor was improved by about one order of that of the sensor for YOHKO. Table 1 shows the UFSS performance requirements for HINODE. Improvements of the performance were achieved by the minimum timing control with an analog delay line. The position resolution of the solar image on

Table 1 UFSS requirements for HINODE

FOV	±0.5 degree
Unobscured FOV requirement	±45 degrees
Data Bit Resolution	0.122 arc sec
Bias error after characterization(Goal)	0.5 arc sec
Random error	2.22 arc sec (3σ)
Temperature Drift	0.5 arc sec/K
Integration time (electrical shutter)	2 ms
Data Update time	16ms
Initial Tracking Time	2 s
Readout cycle time by AUCU	31 ms
Power Interface	50 V unregulated
Power Consumption	6.3 W
Mass	Sensor Hed: 1.2kg Electronics: 1.9kg

*tsuno@riken.jp; phone 81 48 467-9417;
fax +81 48 467-4078; riken.ip

the CCD was improved to 1/256 pixels. The in-orbit performance showed a stability of 0.5 arcsec and a resolution of 0.14 arcsec^[2] in noise equivalent angle (NEA), where the data resolution was 0.12 arcsec. The UFSS has provided sufficient stability and resolution for the X-Ray Telescope (XRT) and EUV Imaging Spectrometer (EIS). Since the spatial resolution of the Solar Optical Telescope (SOT) is about 0.2 arcsec, both the resolution and stability of the UFSS are insufficient for SOT observation. The SOT employed an additional pointing system which stabilized the image based on the granule correlation in time^[3]. The UFSS provided the SOT with an accurate initial observing position on the Sun.

The observing instruments of Solar-C, the next generation solar observation satellite, have been further improved, with a spatial resolution of about 0.1 arcsec, including doubling the aperture of the Solar UV-Visible-IR Telescope (SUVIT). The spatial resolution of the other instruments will be about 0.2 arcsec, a similar resolution to that of the SOT. The satellite system is studied with the UFSS of the same performance as HINODE as a baseline. Fifteen years have passed since the last development of the sun sensor, so the study to reproduce and improve the sun sensor performance has been started. The new mechanical and electronics have been designed considering the update in technology, particularly in semiconductor devices and the reviewing of the previous UFSS thermomechanical design.

2. UFSS DESIGN

2.1 Detection method

The linear CCD sun sensor is one of the most popular attitude sensors in Japanese satellite programs, and 30 units or more have been successfully launched. The sensor detects the position of the projected slit image provided by sunlight, as shown in Figure 1. The solar direction (sun angle) is determined by:

$$\tan \theta = x/h \quad (1)$$

The field of view (FOV) of the sensor is defined by: $\tan \theta_{FOV} = L_{CCD}/2h$, where L_{CCD} is the total length of the linear CCD. A sun angle of higher accuracy is achieved when the position of the image is measured to a higher accuracy or when a larger height h exists between the CCD and the slit. They are very simple but are hard to achieve, mainly due to the following reasons:

- 1) The sensor with an increased h results in a larger sensor body. For a sun sensor as an independent system, it is relatively difficult for the large body to be thermally isolated from the environment. The heat flow generates a significant thermal distortion due to temperature nonuniformity, preventing high accuracy. In order to avoid thermal distortion, the system is installed in a temperature-stabilizing instrument, such as a larger observing telescope. Such sun sensor systems are employed in the XRT on board HINOTORI, not to control satellite attitude but to determine the line of sight (LOS) of the instrument. The system cannot be a general-purpose sun sensor.
- 2) The pixel size is about 14 μm for a standard 2024-pixel linear CCD. In order to achieve high accuracy, the position x will be measured in a sub-pixel dimension. The accuracy of the estimated position is limited by the nonuniformity of the sensitivity and dark signal. For a sensor with $h = 100$ mm, the position determination of 1 μm results in an angular resolution of 2 arcsec. The accuracy of the slit shape also limits the sensor accuracy.

The UFSS was inspired by different ideas, and is a sensor based on the fact that the accuracy can be improved by using the average of data measured by many independent sensors. This method improves the accuracy and resolution by a factor of $N^{-1/2}$ if the error caused by the individual sensors is independent, where N is the number of the slits. Moreover, the effects of a defect of a single slit or of localized pixels can be reduced by a factor of N^{-1} . When multiple slits with equal spacing, a periodic reticle, replace an individual slit, it is equivalent to the multiple sensors formed by each slit and the CCD individual sensors, as shown in Figure 1(b). A higher accuracy can be achieved if the position of the projected reticle image is precisely determined. Contrarily, the projected image on the CCD looks similar to the periodic signal. Rather than detecting the individual image position of slits, the phase of the signal of the reticle can be detected. Though Figure 1(b) shows a sinusoidal image, the actual image is obtained by combining the geometric slit image response, the solar angular image, and the diffraction response; however, this usually produces a distortion.

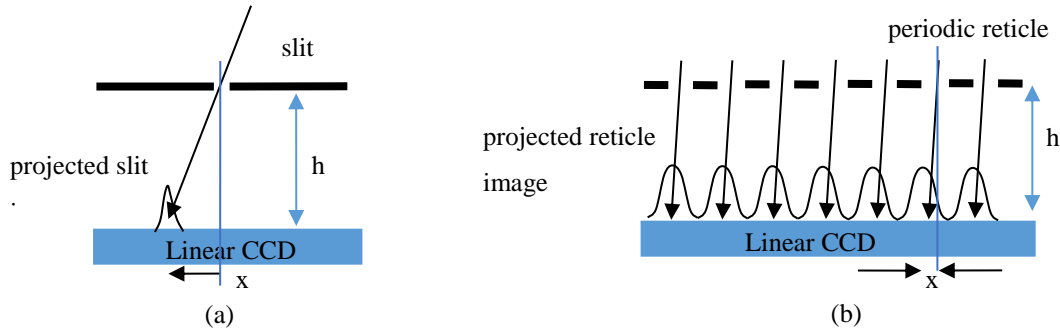


Figure 1. Operation of (a) a simple linear CCD sun sensor and (b) a UFSS

The UFSS uses a method without the effect of distortion of the image. A stable phase reference is required to detect the phase of the signal. The dimension of the CCD, pixel size, and pixel alignment are very precise, of less than a few tens of nanometers, in order to achieve pixel uniformity. The readout timing is also precisely controlled. Therefore, the phase reference shall be generated based on the driving timing of the CCD. This is the best way to measure the phase of the projected image. For example, based on the Fourier series, the phase, i.e., θ in Equation (1), is obtained by the following equations:

$$A \cos \theta = \frac{1}{N} \int_0^{T_R N} \cos\left(2\pi \frac{t}{T_R}\right) \cdot S\left(2\pi \frac{t}{T_R}\right) dt \quad (2)$$

$$A \sin \theta = \frac{1}{N} \int_0^{T_R N} \sin\left(2\pi \frac{t}{T_R}\right) \cdot S\left(2\pi \frac{t}{T_R}\right) dt \quad (3)$$

where T_R is the period of the phase reference signal, and $S(t)$ is the reticle image read out from the CCD. This system detects the phase of the Fourier components with a period T_R of $S(t)$. The above equations were difficult to calculate and solve to obtain θ for small sensor electronics in the 1980s.

When $S(t)$ is a symmetric function of t , the Equation (3) is 0 and can be modified as:

$$A \sin \delta = \frac{1}{N} \int_0^{T_R N} \sin\left(2\pi \frac{t}{T_R} + \theta + \delta\right) \cdot S\left(\pi \frac{t}{T_R} + \theta\right) dt. \quad (4)$$

Equation (4) shows that the phase of the projected image can be detected by adjusting the phase of the correlating sinusoidal function for the equation to be zero. Equation (4) also indicates that there is an error δ of the phase to be adjusted, and when the error is small, it is proportional to the correlation value. Using this, we can take another approach by which the correlation value of Equation (4) can be reduced using feedback techniques. The adjusting function is called a replica function. The replica function does not need to be a sine function, and similar results can be obtained even with a rectangular wave.

$$R(t) = \begin{cases} 1 & 2n\pi \leq t < (2n+1)\pi \\ -1 & (2n-1)\pi \leq t < 2n\pi \end{cases} \quad (5)$$

$R(t)$ and $S(t)$ are expanded respectively and the following result is obtained:

$$\frac{1}{N} \int_0^{T_R N} R\left(2\pi \frac{t}{T_R} + \theta + \delta\right) \cdot S\left(2\pi \frac{t}{T_R} + \theta\right) dt \propto \sum_{n=1}^{\infty} \frac{s_{2n-1}}{2n-1} \sin((2n-1)\delta) \cong \delta \sum_{n=1}^{\infty} s_{2n-1} \quad (6)$$

where s_n is the Fourier coefficient of $S(t) = \sum_{n=1}^{\infty} s_n \cos(t)$.

Finally, the simple rectangular replica function is applicable to retrieve the phase from the projected image, which is easily implemented.

2.2 Electronic design

The phase-retrieving electronics implemented for HINODE are shown in Figure 3. For the design of YOHKOH, the replica signal was simply generated by the MSB of the scaler, for which the spatial period of the reticle was chosen to be 2^n pixels. The 128-pixel period of the 16-slit design was used for the 2048-pixel CCD. The phase was controlled by the initial value

of the scaler designated by the Phase Register (PR), which is the phase-initialized scaler. The value of the PR shows the detected phase, i.e., sun angle, when Equation (6) is equal to zero. The scaler counts synchronously so the phase is not affected by the gate propagating delay. The resolution of the phase is limited by the frequency of the master clock. The speed of the space qualified logic devices in the 1980s was HCMOS, and the master clock frequency was 8 MHz, which corresponded to 1/32 pixel. For the HINODE observatory, the logic devices were small size FPGA. The device speed was not drastically improved. The phase resolution with 1/256 pixel, corresponding to the 64 MHz master clock, was achieved by an 8-tap analog delay line whose maximum delay was set to 1/32 pixel. For the SOLAR-C design, the replica generator is again a simple phase initialized scaler, similar to that for the YOHKOH design, since the FPGA speed is improved to use a 64 MHz master clock.

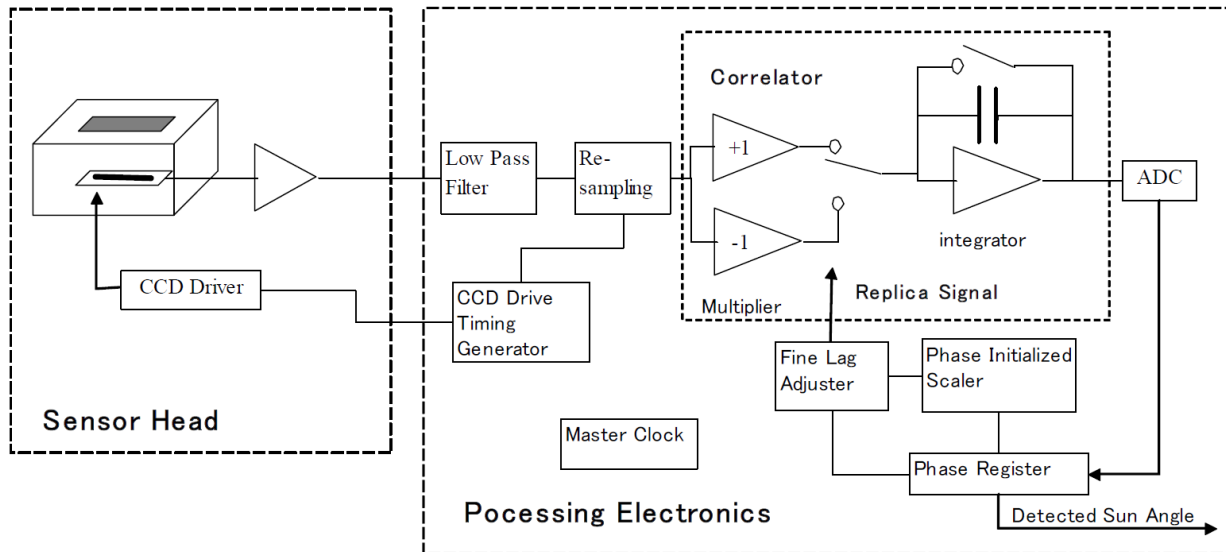


Figure 2. UFSS processing block diagram^[2]

The correlator, the function of Equation (6), is composed of an integrator, analog switch, and amplifiers with a gain of 1 and -1. Since the projected image $S(t)$ is read out from the CCD and processed by separate electronics, the process timing is affected, including by characteristics such as the cable length and frequency response, of the transmission from the CCD to the processing electronics. This effect is caused by mechanical stress, temperature change, and cable length, and may be the cause of the degradation of the stability. The readout signal is quantized temporally in units of CCD pixels. Since the change of characteristics of the transmission line causes a timing deviation from the quantized one, the phase of the projected image deviates. When resampling is performed at the timing synchronized with the CCD driving clock by a sample hold circuit, it is possible to make the deviation a constant delay so that a constant bias is offset in the retrieved phase, therefore not affecting the accuracy and resolution of the sensor.

2.3 Thermomechanical design

The thermomechanical stability is an important aspect of the UFSS. An angle of 1 arcsec corresponds to a displacement of 0.5 μm for a distance of 100 mm. Though the orbital temperature variation of the sensor shall be interfaced to be less than 1 K, it is not a negligible change in terms of sensor stability. The submicron mechanical stability for a 1 K deviation is required in orbit.

For a body with a uniform coefficient of thermal expansion (CTE), the body does not bend or distort but only deforms similarly when it has a uniform temperature distribution. Dimensional differences between objects with different temperatures or CTEs are supported by kinematic mounts so that the angular displacement is minimized. Fourier's law of thermal conduction, $\vec{q} = -\kappa \text{grad}(T)$, where \vec{q} is the heat flux, shows that any heat flux generates a temperature gradient. Therefore, the stable system shall be thermally isolated and have less heat sources in order to minimize thermal

distortion. The HINODE UFSS was thermomechanically designed according to the above approach. For the SOLAR-C project, the UFSS design will be improved based on HINODE heritage.

- (1) The main structure, or optical bench, is made by a monolithic titanium alloy with a close CTE to the CCD package and the reticle.
- (2) The optical bench is supported by kinematic mounts to isolate it from distortion of the mounting points and bottom and top chassis.
- (3) The CCD, which generates 0.1 W, is mounted by a thermal isolator and the generated heat will be transported to the mounting point through a flexible laminated copper thin film so that heat does not flow through the optical bench.
- (4) The electronics PCB, which includes the CCD driver and proximity amplifier, is mounted on the bottom chassis and its heat is transported in the bottom chassis.
- (5) Injected heat by solar radiation is absorbed at the top chassis and ND filters are transferred through the top chassis to the mounting points to avoid transferring through the optical bench.

In addition, it is devised so the CCD and the reticle are positioned at the center of the effective length, since the symmetrical expansion with respect to their center has no primary effect on the detected angle.

The stability is finally verified by thermomechanical FEM analysis to satisfy the LOS stability, the design strategy is crucial in minimizing the distortion.

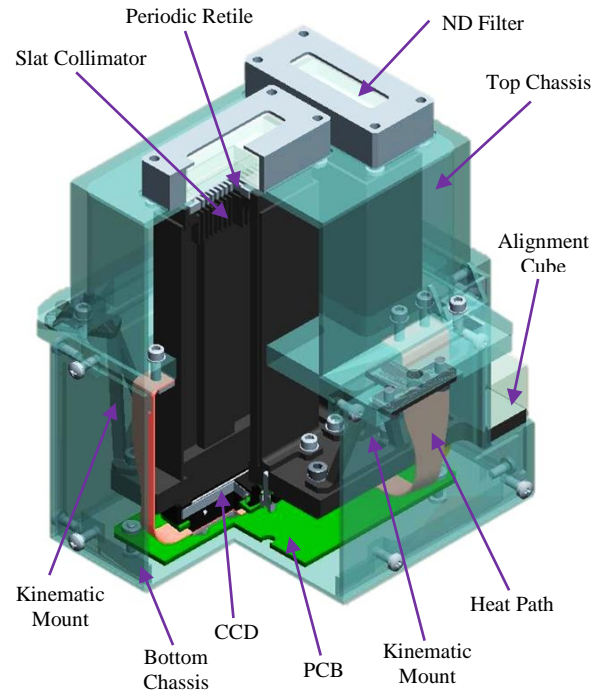


Figure 3. SOLAR-C UFSS Mechanical Structure

3. ANALYSIS AND CHARACTERIZATION OF OPERATION

The processing algorithms are the same for both the YOHKOH and HINODE sensors.

Assuming that the value of the PR is P_n at the n -th CCD scanning period, the Correlator output C_n denotes the ADC output, which is obtained according to Equation (6) by the scanning CCD. The PR is updated by:

$$P_{n+1} = P_n - C_n. \quad (7)$$

P_n and C_n have integer values with the finest resolution, LSB, of the phase as a unit. When C_n is small, it can be linearized as $C_n = k(P_n - \theta)$ and $P_{n+1} = P_n - k(P_n - \theta)$ can be obtained, where k is the feedback gain.

Assume $E_n = P_n - \theta$, E_n indicates the detected phase error, then Equation (7) can be modified to give the relationship of the phase error:

$$E_{n+1} = (1 - k)E_n. \quad (8)$$

This recurrence formula is easily solved and the following result is obtained:

$$E_n = E_0(1 - k)^n. \quad (9)$$

When $|1 - k| < 1$, the detected phase error converges to zero. Feedback gain is a very important parameter. In more

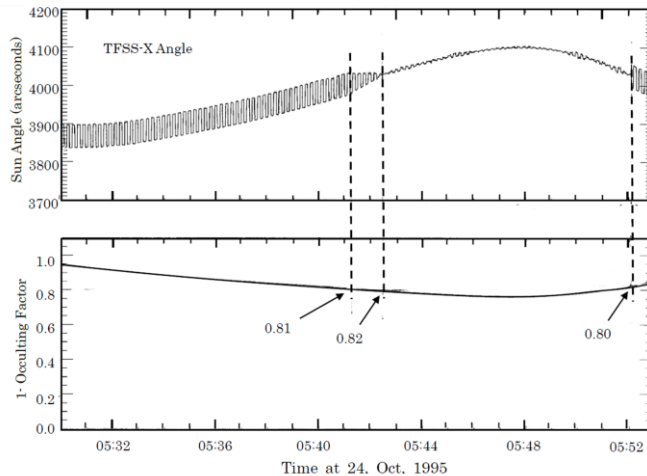


Figure 4. YOHKOH flight data during a solar eclipse

detail; it monotonously decreases when k changes from 0 to 1, and damped oscillation occurs for values of k from 1 to 2, however, when k is 2 or more, it vibrates divergently. For smaller k , less than 1, the system is guaranteed to be stable. However, due to integer processing, P_{n+1} in Equation (7) does not update when C_n is a fractional value. The residual error, which is the phase difference between the projected image and the replica signal, at this time is expected to be a maximum of $1/k$.

In the YOHKOH sensor, a problem occurred due to the selection of the feedback gain. The feedback gain k was designed to be 1 to minimize the processing residual error. Since the field of view of the sensor was set to be wider than that of HINODE, the image of the reticle was hardly affected by smoothing of the solar image, and has a near-rectangular shape more than a sinusoidal one. As a result, according to Equation (6), the feedback gain was about 30% larger than in the case of the sinusoidal image. Based on the field test using sunlight, the adjustment of the transmission of a neutral density filter was accidentally selected to be larger value. As a result, k was selected to be larger than 2, and the detection logic oscillated in orbit. In this case, the feedback value C_n was limited to a 6-bit value, from -31 to 32, the system showed the limit cycle oscillation with an amplitude of 31 in peak-to-peak and a period of 2 times the processing period. Figure 4 shows the in-orbit data of the YOHKOH sun sensor, TFSS, during a solar eclipse. The amplitude of the projected reticle image was approximately equal to the residual area of the apparent solar surface when the sun was occulted, given by “1-Occulting Factor” in the figure. The oscillation had a peak-to-peak amplitude of 31 digits, about 60 arcsec and a frequency of about 0.08 Hz. This frequency is considered to be the aliasing effect, caused by the low-sampling frequency of the telemetry on the fast updating sensor of 125 Hz. The system is stable when the amplitude of the reticle image is about 0.8 or less, $k < 2$. In the case of $k \sim 2$, it is expected that the stability of the system is limited in response to a small external disturbance. So, once oscillation occurs it is difficult to stop, and oscillation from the stable state starts promptly by the external disturbances. For the YOHKOH sensor, the feedback gain was estimated to be 2.5. Fortunately, the oscillating amplitude, 31 digits peak-to-peak, was so stable that the filtering in the attitude control system provide enough accuracy and resolution for YOHKOH observation.

Since this sun sensor consists of such a control system, it seems to be meaningful to investigate its dynamic characteristics. When the discrete system of Equation (8) is approximated by a continuous system, the relationship given by Equation (10) is obtained:

$$\frac{d\varepsilon(t)}{dt} = -k\varepsilon(t) + k\Delta(t) \quad (10)$$

where the temporal function $\Delta(t)$ is the input of disturbance, such as a change in spacecraft attitude or noise; $\varepsilon(t)$ is the response readout sensor data. The transfer function $H(s)$ is given as the first-order lag system with a cutoff frequency of k .

$$H(s) = \frac{1}{1 + \frac{s}{k}} \quad (11)$$

When the HINODE sun sensor was designed, the stability tended to be lost if the amplitude of the projected reticle image was too large. The tradeoff of the risk of convergence residuals against stability was, hence, studied. It was designed as $k = 0.5$ to 1 to reduce the risk of losing stability. This selection is justified by a phase resolution of the replica signal of $1/8$, given by the delay line technique, and the resolution in RMS limited by the photon shot noise of the CCD becomes almost equal to the LSB of PR, the control residual can be ignored. In-orbit data shows an NEA of 0.14 arcsec. Considering an LSB of 0.12 arcsec,^[2] the HINODE UFSS reached maximum NEA performance, limited by the CCD performance with a maximum temporal resolution; it is not necessary to further improve the phase control resolution of the replica signal using a higher frequency clock. However, the data update of the UFSS is about 10 Hz, and by devising a CCD readout method,

it is possible to increase the speed to about 100 Hz, since the line readout is completed in 8 ms. Considering that the system is a first-order lag system, the above averaging effect can be installed in the sensor by adjusting the response speed of the system, $1/k$. Although there is a possibility that the NEA can be small, the phase resolution of the replica signal does not change and the residual error becomes large, so it cannot be directly applied to the HINODE system.

Following the simple modifications may archive both the reduction of the residual error and reduction of the NEA. The PR should be a fixed-point real number whose integer part should control the replica signal and C_n shall also be a fixed-point real number. The LSB of the ADC output shall be modified to be the LSB of the fractional part. Since the CCD shot noise is random, it can be expected that the noise decreases in proportion to $k^{1/2}$ according to the decrease of the bandwidth k . The phase resolution of the replica signal is limited by only the integer part of the PR. Since the error caused by the fractional part is a quantization error with a standard deviation σ_p of $1/\sqrt{12}$ LSB, the random error due to the CCD noise σ_{CCD} shall be large enough to ignore the quantization effect, empirically $\sigma_p > 3\sigma_{CCD}$. Figure 5 shows the simulation results with $k = 0.125$, $\sigma_{CCD} = 1$. The vertical unit of the figure is the minimum phase resolution of the replica signal and the vertical unit is the updated cycle. The step response shows a time constant of 8, and a residual error of 0.24 RMS. The NEA will be about 3 times smaller than σ_{CCD} . The residual error has a significant offset which is a constant offset caused by the truncated fraction of the PR. The result shows the possibility for an improvement of the UFSS NEA of about 0.05 arcsec.

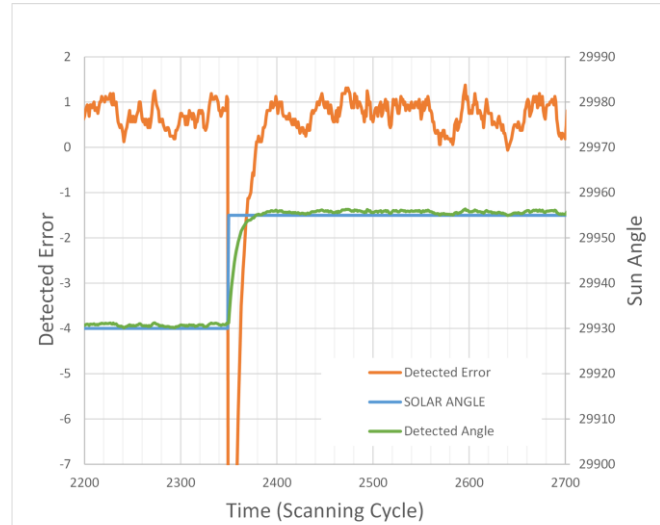


Figure 5. Step response simulation result of UFSS. Vertical unit is shown by the minimum phase resolution unit.

4. CONCLUSION

The YOHKOH and HINODE sun sensors were reviewed and analyzed. The stability condition of the system was obtained, which may explain the malfunctions of the YOHKOH flight system. The dynamic characteristics of the sun sensor data are characterized by the first-order lag system and the following simple modifications for the SOLAR-C UFSS are proposed to improve the NEA performance up to 0.05 arcsec:

- The PR, which shows the sun angle, shall have an additional fractional 4 bits.
- The ADC-conversion LSB shall be adjusted to that of the PR.
- The feedback gain k shall be 0.125 (= 1/8).

The thermomechanical design was also studied and can be verified by FEM analysis and by a hardware model. Even if the stability caused by a temperature change cannot be greatly improved from the HINODE UFSS, a short-term stability of 0.1 arcsec is expected within 10 min based on HINODE data. When an NEA of 0.05 arcsec is achieved, the UFSS may be a candidate for the backup system of the pointing system with a high-resolution optical telescope for observation.

The BBM electronics and structure were completed to verify the design study.

Another important issue in the development of a ultra-high precision sun sensor is verification^[4]. Since an accurate verification of the equipment in the HINODE project, as well as the UFSS, is required, many trial and error and a final test of several months were required. Using the assembled BBM, we are also planning a compatibility and evaluation of BBM with the improved test system.

ACKNOWLEDGEMENTS

The authors would like to express our sincere gratitude to Mr. T. Okamoto and Mr. S. Akabane who were YOHKOH sensor engineers, and Mr. T. Okumura and Mr. T. Yamamoto who were HINODE sensor engineers. They are also grateful to Dr. K. Ninomiya and Mr. T. Kameda who provided the opportunity to create the idea of periodic reticle sun sensors.

REFERENCES

- [1] Niomiya, K., Ogawara, Y., Tsuno, K., and Akabane, S., "High accuracy sun sensor using CCDs," Technical Papers in AIAA Guidance, Navigation and Control Conference, Minneapolis, August 1988, Part 2, 1061–1070 (A88-50160-21-08).
- [2] Tsuno, K., Yamamoto, T., Kubo, M., Shimizu, Y., Hirokawa, E., and Hashimoto, T., "CCD sun sensors on board 'Hinode' solar observatory," Proc. ICSO 2008, Poster for Auxiliary Sensors.
- [3] Kodeki, K., Kashiwagi, Y., et al., "Development of a correlation tracker and a tip-tilt mirror system for SOLAR-B," J. JSASS 55 (637), 57–64 (2007).
- [4] Kubo, M., Shimizu, T., et al. "Performance verification of Ultra Fine Sun Sensors (UFSS) aboard HINODE," JAXA Research and Development Report, JAXA-RR-07-013, 1–13 (2008)